International Journal of Technology 14(1) 15-25 (2023)
Received August 2021 / Revised February 2022 / Accepted July 2022

International Journal of Technology

Cyclic Oxidation Resistance of $MoSi_2$ Added FeCrAlTiY Coatings on ST41 Steel at 700°C Prepared by a Flame Spraying Technique

Januaris Pane[1,3], Dedi Holden Simbolon[1,4], Hubby Izzudin[2], Ahmad Afandi[2], Bambang Hermanto[2], Kerista Sebayang[1], Syahrul Humaidi[1], Marhaposan Situmorang[1], Toto Sudiro[2*]

[1]*Postgraduate Program of Physics, Faculty of Mathematic and Natural Science, Universitas Sumatera Utara, North Sumatera 20155-Indonesia*
[2]*Research Center for Advanced Material, National Research and Innovation Agency, Kompleks PUSPIPTEK Serpong, South Tangerang, Banten 15310-Indonesia*
[3]*Pendidikan Fisika, FKIP, Universitas HKBP Nommensen Medan, North Sumatera 20234-Indonesia*
[4]*Department of Primary School Teacher Education, FKIP, Universitas Quality, North Sumatera 20132-Indonesia*

Abstract. Advanced power generation will be operated at higher temperatures and pressure to achieve higher efficiency and reduce CO_2 emission. This may significantly impact the use of carbon steel that previously has been used in boiler fabrication. In this study, a flame spraying technique was applied to develop a highly resistant coating of $MoSi_2$ added FeCrAlTiY on ST41 steel to improve its oxidation resistance. Four variations of $MoSi_2$ concentration as 0, 10, 20 and 30 in mass% were prepared to investigate the effect of its addition on the cyclic oxidation resistance of FeCrAlTiY coating at 700°C for 8 cycles. The phase composition and microstructure of the coating before and after the oxidation test were analyzed using XRD and SEM, respectively. While the element distribution along the coating was characterized using an EDX. According to the results, partially and fully melted particles, oxides and pores are present in the coatings. It becomes more porous with the increase of $MoSi_2$ concentration. The oxidation test results indicate that the FeCrAlTiY with 10 mass% $MoSi_2$ addition exhibits the lowest mass gain (0.217 mg/mm^2) compared to that of $MoSi_2$-free coating (0.261 mg/mm^2) and FeCrAlTiY coating with 20 and 30 mass% $MoSi_2$ (0.297 and 0.308 mg/mm^2, respectively). As the $MoSi_2$ concentration increases, its addition leads to the deterioration of FeCrAlTiY coating oxidation resistance. The results suggest that FeCrAlTiY-10 mass% $MoSi_2$ is the most resistant coating to cyclic oxidation at 700°C in air and can be applied as a protective coating in advanced power generation.

Keywords: Carbon Steel; FeCrAlTiY; Flame Spraying; $MoSi_2$; Oxidation

1. Introduction

In order to achieve higher efficiency and reduce CO_2 emissions, the working fluid of the boiler will be operated at higher temperatures and pressures. In the next decade, Advanced ultra-supercritical power plants (A-USC) are expected to enter operation and will approach 50% net electricity generation efficiency with the use of advanced metal alloys capable of withstanding steam temperatures and pressures over 700°C and 350 bar (Tramošljika *et al.,* 2021). The usage of carbon steels that are widely used for a wide range

*Corresponding author's email: toto009@brin.go.id, Tel.: +62 21 7560556, Fax: +62 21 7560554
doi: 10.14716/ijtech.v14i1.5092

of industrial applications, such as boiler and pressure vessel fabrication, may become limited when applied at high temperatures and oxidative atmospheres. The Fe element tends to be easily oxidized to form thick Fe-oxide layers. Accordingly, surface treatment is required (Simbolon *et al.,* 2020).

It is well known that surface structure modification as surface hardening (Ismail and Taha, 2014) and coating deposition has been widely used to reduce part production costs (Luo *et al.,* 2014), to improve wear resistance, hardness, or to act as environmental barrier coating (EBC) for critical components, resulting in higher oxidation or corrosion resistance (Singh *et al.,* 2022). Thus, the selection of appropriate coating material and composition becomes particularly important (Saraswati, Nugroho, and Anwar, 2018). The FeCrAlY was receiving attractive attention for high-temperature oxidation and corrosion resistance applications because of the formation of a protective scale in the external layer (Wessel *et al.,* 2004; Bennett and Bull, 1997). In addition, the selection of the appropriate coating method largely determines the final coating properties. Thermal spray technology as HVOF and flame spraying, offers some advantages, including it can be applied for various kinds of materials, creating near net shapes of nanostructured or nanocomposite, and also being easy to use (Simbolon *et al.,* 2020; Sofyan *et al.,* 2010).

In order to solve the aforementioned issues, alloying elements may be added to the mix. Several studies have reported the beneficial effect of some elements as Si and Mo, in improving the properties of metals and alloys. Inoue *et al.* (2018) reported that an adequate amount of Si addition to stainless steel could promote the formation of SiO_2 layer at the substrate/oxide interface. The formed SiO_2 can also act as the nucleation site for the formation of Cr_2O_3 scales (Nikrooz *et al.,* 2012). Saito *et al.* (1998) also pointed out that the crystalline SiO_2 can act as a heterogeneous nucleation site and accelerates the γ-Al_2O_3 to α-Al_2O_3 transformation. While the appropriate amount of Mo content has beneficial effects in improving oxidation resistance (Yao *et al.,* 1999). Many researchers have shown an increased interest in attractive silicides material of $MoSi_2$ for high-temperature resistance applications due to its properties such as high melting temperature, low density, high hardness and excellent oxidation resistance (Wen and Sha, 2018; Zhang *et al.,* 2019).

Based on the points presented above, this paper attempts to consider the addition of $MoSi_2$ to improve the FeCrAlTiY oxidation resistance. The primary aim of the present work is to investigate the effect of $MoSi_2$ addition on the high-temperature oxidation behavior of flame-sprayed FeCrAlTiY coatings deposited on the surface of low carbon steel at 700°C.

2. Materials and Methods

FeCrAlTiY-$MoSi_2$ coatings on carbon steel ST41 were prepared by using a flame spray technique. The sample and coating preparation procedures were conducted according to our previous study (Simbolon *et al.,* 2020). Here, we briefly repeated the experiment. The commercial ST41 steel was cut into coupons of about 10 × 10 × 3 mm (see Figure 1a). A hole was made in the top part of the sample to hang it during the coating process. The substrate surface was ground to SiC papers and cleaned in an ultrasonic bath using an ethanol solution. It was dried and then sandblasted using coarse brown fused alumina.

The commercial powders of FeCrAlTiY-Sandvik Materials Technology Ltd. (Fe, 17.2 Cr, 6.6 Al, 0.58 Ti, 0.47 Ni, 0.36 Mn, 0.097 Y, 0.097 Cu) with an average size of about 106 μm and $MoSi_2$-Japan New Metals Co. Ltd. (Mo, 35.8-37.8 Si, ≤ 0.05 C, ≤ 0.23 Fe, ≤ 0.5 O) with the average size of about 5~10 μm were selected as powder coating. To investigate the influence of $MoSi_2$ content on the oxidation resistance of FeCrAlTiY coatings, four different coating compositions such as FeCrAlTiY coating with 0, 10, 20 and 30 mass % $MoSi_2$ were deposited on the all surfaces of ST41 (see Figure 1b) using a Metallisation Flamespray

MK74. Before coating, each composition was mixed by rotary milling for 30 min. Here, the pressure of oxygen and acetylene for coating deposition was adjusted to 2.07 and 0.83 bars, respectively and the compressed air pressure was set to 1.34 bars. The distance between the sample and the spray gun was kept constant carefully of about 20 cm.

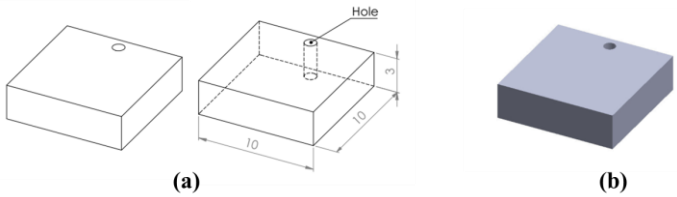

Figure 1 The schematic images of (a) ST41 without coating and (b) FeCrAlTiY-$MoSi_2$ coatings on ST41

The resistance of coatings toward oxidation at high temperatures was evaluated according to the mass gain of the oxidized sample. All coated samples were placed in an alumina crucible separately. The samples were then cyclically oxidized in static air of a muffle furnace at 700°C eight times. One cycle consists of 20 h exposure at 700°C, and 4 h cooled down to room temperature. The mass gain of the samples at each cyclic time was periodically measured using an electronic balance with an accuracy of 0.01 mg. The aforesaid temperature was chosen to represent the operational temperature of A-USC.

The phase composition of the coatings was determined by using X-ray diffraction (Rigaku Smartlab). In order to examine the oxide scales formed on the coating surface, the XRD analysis was performed on the oxidized surface. The microstructure evolution and compositional analysis of cross-sectional samples were investigated using a scanning electron microscope (SEM Hitachi SU3500) and energy dispersive X-ray spectrometer (EDX Horiba), respectively. In this study, the microstructure of oxidized coated sample was also compared with the substrate without a coating which was oxidized with the same conditions as described above.

3. Results and Discussion

3.1. XRD and SEM Analysis of FeCrAlTiY and $MoSi_2$ Powders

The X-ray diffraction patterns and the SE SEM images of FeCrAlTiY and $MoSi_2$ powders used in this study are presented in Figure 2 and 3, respectively.

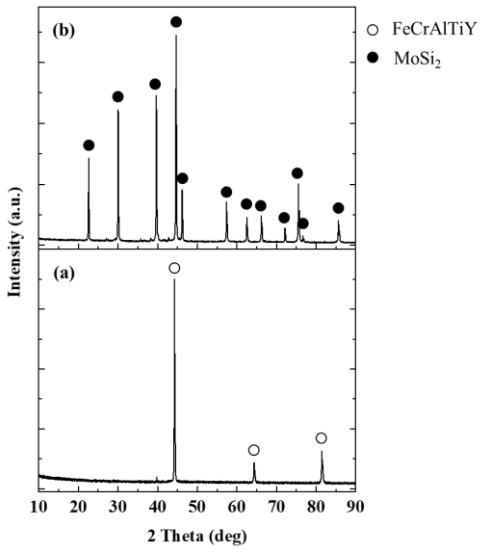

Figure 2 X-ray diffraction patterns of (a) FeCrAlTiY and (b) $MoSi_2$ powders

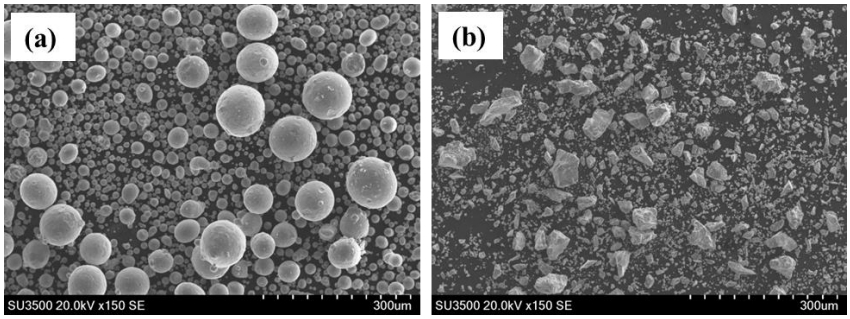

Figure 3 SE SEM images of (a) FeCrAlTiY and (b) $MoSi_2$ powders

It can be seen that the original FeCrAlTiY and $MoSi_2$ powders show spherical and irregular morphology, respectively.

3.2. Phase Constituent and Microstructure of FeCrAlTiY-$MoSi_2$ Coatings

The phase structures of FeCrAlTiY-$MoSi_2$ coatings on ST41 are shown in Figure 4. The FeCrAlTiY coating without $MoSi_2$ addition is composed by FeCr [DB Card No.: 00-034-0396], Fe(Cr, Al)$_2O_4$ [DB Card No.: 00-003-0873] and FeO [DB Card No.: 00-074-1884]. Meanwhile, other new phases such as $MoSi_2$ [DB Card No.: 00-081-2167] and Mo_5Si_3 [DB Card No.: 00-008-0429] are found in the FeCrAlTiY coating with different content of $MoSi_2$. The intensity of the FeCr phase in the coatings tends to decrease with the addition of $MoSi_2$. In contrast, the oxides of Fe, Cr and Al are likely to form in the coating. This could be due to the fact that the oxides are covering the metallic compounds. The presence of oxides in the coating implies that some coating elements are more favored to oxidize during coating preparation to form FeO and Fe(Cr, Al)$_2O_4$. It seems that Al_2O_3 and Cr_2O_3 scales were formed firstly during flame spraying because of a strong affinity of Al and Cr for oxygen. The consumption of Al and Cr leads to its coating element depletion. Accordingly, the Fe element was then preferentially oxidized to form FeO. Some amount of FeO was then reacted with Al_2O_3, Cr_2O_3 and oxygen, forming Fe(Cr, Al)$_2O_4$.

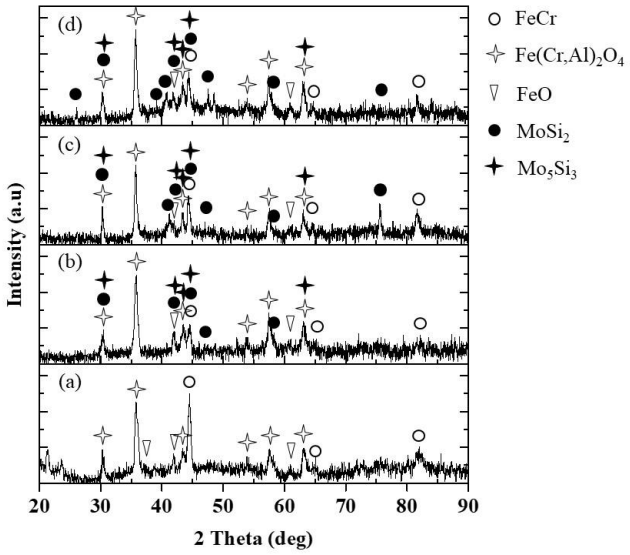

Figure 4 XRD patterns of FeCrAlTiY coatings with (a) 0, (b) 10, (c) 20 and (d) 30 mass% $MoSi_2$

It is worth noting that the Mo_5Si_3 phase with intensity difference is observed in the FeCrAlTiY-$MoSi_2$ coatings. Its formation may proceed due to the oxidation reaction of the $MoSi_2$ phase through the following reaction,

$$5\ MoSi_2 + 7\ O_2(g) \rightarrow 7\ SiO_2 + Mo_5Si_3 \quad (1)$$

as reported by previous studies (Zhu *et al.*, 2022; Hansson *et al.*, 2004). Si from the $MoSi_2$ phase was consumed and reacted with oxygen to form SiO_2 and Mo_5Si_3. However, as shown in Figure 4 b, c and d, the SiO_2 peaks' reflection is not observed. This may be attributed to the fact that the oxide is in the amorphous phase, so it is not detected by X-ray diffraction (Chakraborty, 2016).

Figure 5 shows the typical SEM cross-sectional microstructures of FeCrAlTiY-$MoSi_2$ sprayed coatings on low carbon steel using the flame spray technique.

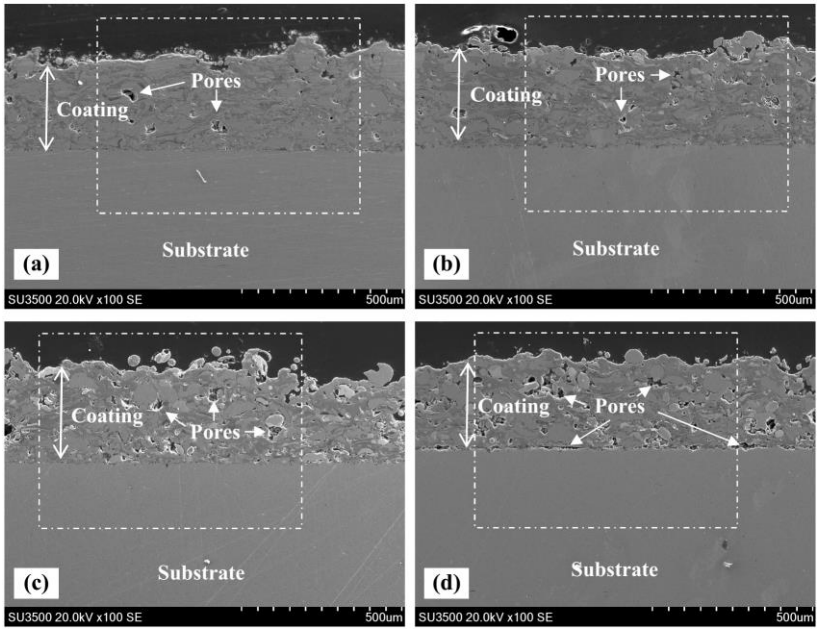

Figure 5 Cross-sectional SE SEM images of FeCrAlTiY coatings with (a) 0, (b) 10, (c) 20 and (d) 30 mass% $MoSi_2$

The thickness of the coating is about 280-350 µm. According to the cross-sectional images, as shown in Figure 5, the coating appears to have typical lamellar structures of thermal spray coating containing fully melted particles and partially deformed particles, oxides and pores. From Figure 5b, c and d, it can also be seen that with the increase of $MoSi_2$ content, the coatings are susceptible to pores formation. This might be related to the high melting point of $MoSi_2$ (Wen and Sha, 2018). The existence of unmelted, partially, and resolidified particles melted particles creates pores within the coating (Khalesi *et al.*, 2021). It can be seen that 30 $MoSi_2$ addition essentially changes the coating microstructure. Pores are also found at the coating/substrate interface. Mostly, the coating porosity and adherence will significantly affect its oxidation resistance. The presence of pores and cracks can act as a short circuit path for inward oxygen diffusion, resulting in reducing the sample oxidation resistance.

To examine the distribution of elements in the FeCrAlTiY-$MoSi_2$ coatings, we performed BSE SEM and EDX elemental maps analysis in the white striped area of Figure 5, with the results as presented in Figure 6. Mostly, the BSE comp image of black, dark and bright areas indicates pore, oxide and metallic phases, respectively. From EDX elemental maps of FeCrAlTiY coating with different content of $MoSi_2$, one of the results show the presence of oxygen distribution in the coating as a mark with green color which reveals that some coating elements are already oxidized during coating preparation, supporting the results of the XRD analysis as explained above. As shown in Figure 6a, the coating is mostly composed of dark areas and bright areas. The dark area consists of Fe, Cr, Al and O (See Figure 6a). It

seems to be $Fe(Cr, Al)_2O_4$ and FeO phases according to the results of X-ray diffraction analysis. The grey area is composed mainly of Fe and Cr, with a trace amount of Al that should be the FeCr phase containing Al.

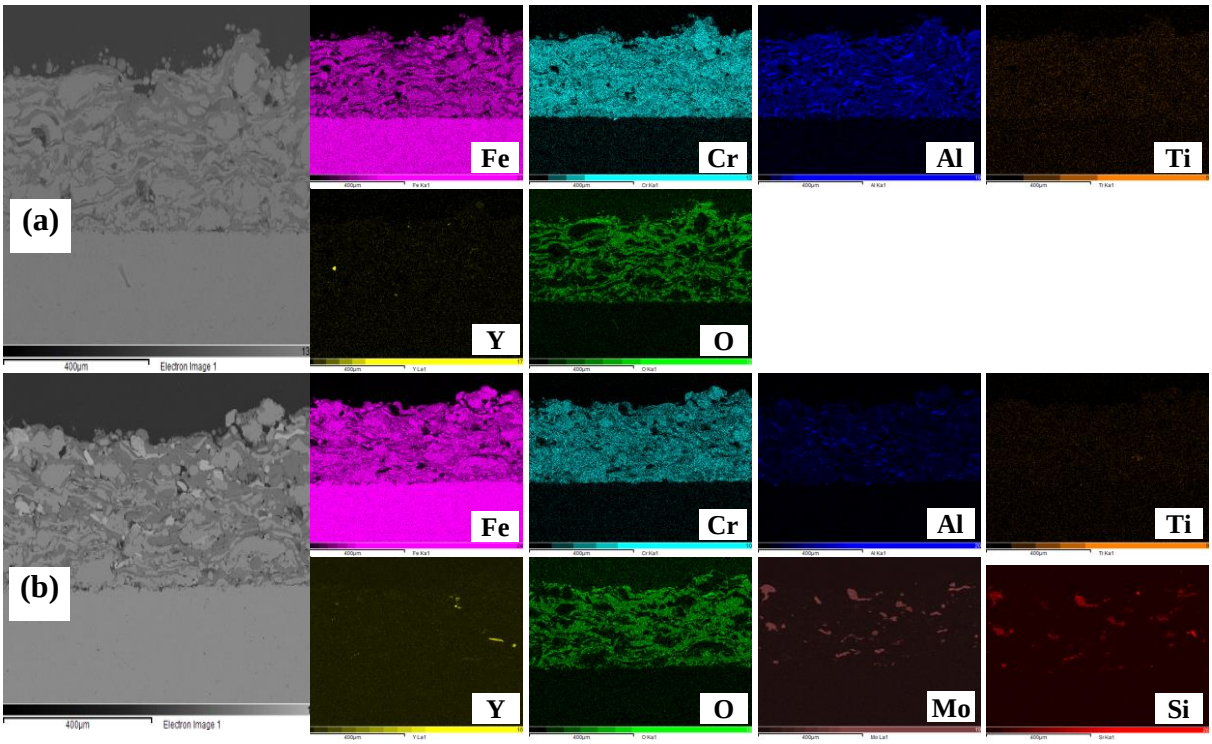

Figure 6 The cross-sectional BSE SEM images and corresponding EDX elemental maps of FeCrAlTiY coatings with (a) 0 and (b) 10 mass% $MoSi_2$

Meanwhile, the microstructure of FeCrAlTiY coatings with 10, 20 and 30 mass% $MoSi_2$ coatings is almost similar to that of $MoSi_2$-free coating that consists mainly of a dark area of Fe, Cr, Al and O, and the grey area of Fe, Cr and Al, for example, as shown in Figure 6(b) for 10 mass% $MoSi_2$ addition. A bright area of Mo and Si is observed in FeCrAlTiY coatings with varying amounts of $MoSi_2$ that are suspected to be $MoSi_2$ and Mo_5Si_3 phases. Mo_5Si_3 usually forms at the SiO_2 and $MoSi_2$ interface due to Si consumption (Hansson *et al.,* 2004). However, it is important to note that in the external layer of 30 mass% $MoSi_2$ coatings, a continuous oxygen distribution can be distinguished. This is one indication that the surface of FeCrAlTiY-30 mass% $MoSi_2$ coating is covered by an oxide layer that formed during coating preparation. Even if the formation of oxide during coating preparation prefers to be avoided, its formation may give a potential benefit in providing temporary oxidation protection.

3.3. Oxidation Behavior of FeCrAlTiY-$MoSi_2$ Coatings

Figures 7a and b compare the mass gain per unit area and the square of mass gain per unit area of the FeCrAlTiY-$MoSi_2$ coatings as a function of cyclic oxidation time exposed at 700°C for up to 8 cycles in air atmosphere. The results as shown in Figure 7a show a clear trend of an increasing mass gain of FeCrAlTiY-$MoSi_2$ coatings along the oxidation period. In the initial stage of oxidation, the increase of mass gain is high until the oxide scale is developed on the external layer. Subsequently, the increase of mass gain tends to be slow because the growth of the oxide layer is controlled by cations and anions diffusion across the oxide layer. It can be seen in Figure 7b that the square of mass gain per unit area of the samples tends to increase linearly with cyclic oxidation time, suggesting that the oxidation of FeCrAlTiY-$MoSi_2$ coating obeys the parabolic rate law.

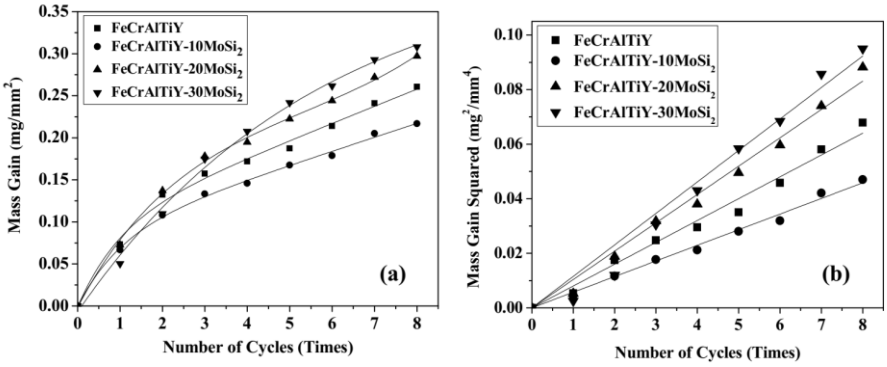

Figure 7 The mass gain per unit areas and square of mass gain per unit areas of FeCrAlTiY $MoSi_2$ coatings after exposure at 700°C for 8 cycles in air

The oxidation kinetic of FeCrAlTiY coatings varied depending on $MoSi_2$ concentration. For 100% FeCrAlTiY coating, the mass gain of the sample is about 0.261 mg/mm^2. The 10 mass% $MoSi_2$ addition leads to lowering the mass gain of FeCrAlTiY coating to 0.217 mg/mm^2. In contrast, the addition of 20 and 30 mass% $MoSi_2$ appears to enhance the mass gain of FeCrAlTiY coating into 0.297 and 0.308 mg/mm^2, respectively. The mass gain of 30 $MoSi_2$ addition is smaller compared to the other components in the first cycle. It then gradually increases for up to eight cycles, resulting in a larger mass gain than other coatings. This is probably due to the formation of the external oxide layer on the FeCrAlTiY-30$MoSi_2$ coating plays a role in providing temporary protection in the initial stage of oxidation. However, after a certain time of exposure, the oxide layer was degraded, promoting accelerated oxidation. As a result, the mass gain of 30 mass% $MoSi_2$ coating is higher than the other samples. The results, as presented above, suggest that 20 and 30 mass% $MoSi_2$ additions are considerably worse to the oxidation resistance of FeCrAlTiY coating. Meanwhile, the addition of 10 mass% $MoSi_2$ has a beneficial effect in improving the oxidation resistance of FeCrAlTiY coating.

3.4. Phase Constituent and Microstructure of FeCrAlTiY-$MoSi_2$ Coatings After Oxidation

Figure 8 shows the XRD patterns of FeCrAlTiY-$MoSi_2$ coatings fabricated by a flame spray technique oxidized at 700°C for 8 cycles. The XRD measurement was performed on the surface of the oxidized coating.

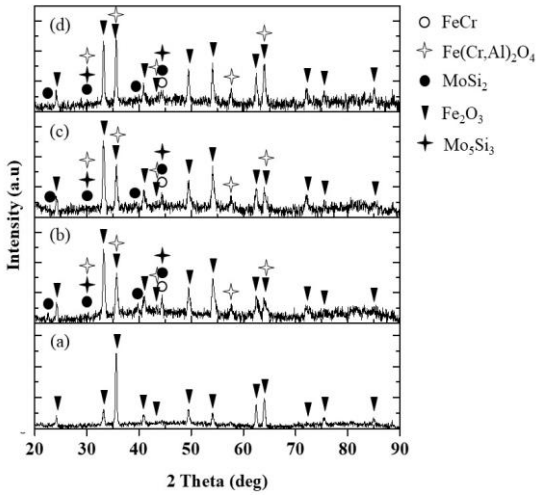

Figure 8 XRD patterns of FeCrAlTiY coatings with (a) 0, (b) 10, (c) 20 and (d) 30 mass% $MoSi_2$ after exposure at 700°C for 8 cycles in air

The main phase was detected in the FeCrAlTiY coating after oxidation, namely Fe_2O_3 [DB Card No.: 00-080-2377]. The reflection of coating peaks is not detected in Figure 8a.

This is due to a thickening of the oxide layer in the external layer of FeCrAlTiY coating. As a result, X-ray diffraction could not reach the coating surface. On the other hand, there is no significant difference in the coating structure of FeCrAlTiY coating with 10, 20 and 30 mass% $MoSi_2$ after exposure at 700°C for 8 cycles. The coatings form Fe_2O_3 and $Fe(Cr, Al)_2O_4$ after oxidation. The peak coating reflection as FeCr, $MoSi_2$ and Mo_5Si_3 can still be observed, as shown in Figure 8 b, c and d. But it tends to decrease with the increase of $MoSi_2$ addition in the coatings. This evidence suggests that the oxide scale of FeCrAlTiY coating without $MoSi_2$ addition is thicker than that of $MoSi_2$ addition coatings. Moreover, as $MoSi_2$ content in the coating increase from 10 to 30 mass%, the thickness of the oxide layer is likely to increase.

The microstructure transformation of FeCrAlTiY-$MoSi_2$ coatings after the oxidation test at 700°C for 8 cycles can be observed in Figure 9. It can be seen in 100% FeCrAlTiY coating a thick oxide layer with a thickness of about 130 µm is formed on the coating surface, resulting in a high sample mass gain compared to the 10 mass% $MoSi_2$ coatings. A severe crack formation is also observed in the formed oxide layer and at the oxide/coating interface. In addition, similarly to the other coating composition, pores are still found within the coating layer. The presence of cracks and interconnected pores can act as freeways or paths for the oxidizing gases to penetrate and/or cation diffusion in the coating, oxidizing it and accelerating its degradation (Simbolon *et al.*, 2020; Esmaeil, Nicolaie, and Shrikant, 2019a; Esmaeil, Nicolaie, and Shrikant, 2019b).

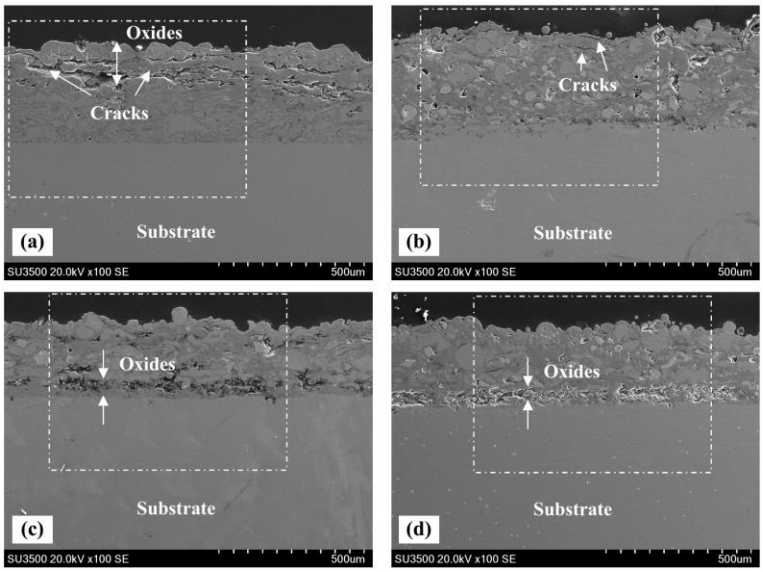

Figure 9 Cross-sectional SE SEM images of FeCrAlTiY coatings with (a) 0, (b) 10, (c) 20 and (d) 30 mass% $MoSi_2$

With the addition of $MoSi_2$, the coatings exhibit less severe oxide crack formation on their surface. The oxide layer of $MoSi_2$ coatings is thinner compared to that of 100% FeCrAlTiY coating. However, in the 20 and 30 $MoSi_2$ coatings, oxidation is also favour to occur at the substrate interface, suggesting the oxygen potential is high at this location. This is related to the more porous microstructure of 20 and 30 $MoSi_2$ coatings before oxidation (see Figure 5). Oxygen is more easily diffused inwardly, leading to oxidation at the substrate interface. This is also the reason why the mass gain of 20 and 30 $MoSi_2$ coatings is higher than the 10 $MoSi_2$ coating.

Figure 10 shows the cross-sectional BSE SEM images and corresponding EDX elemental maps of carbon steel and FeCrAlTiY-$MoSi_2$ coatings after oxidation at 700°C for 8 cycles.

As shown in Fig 10(a), at 700°C, the ST41 experienced a high oxidation rate. The carbon steel is highly consumed, forming thick iron oxide layer on the steel surface. Meanwhile, as can be seen in Figure 10(b) and 10(c), the external layer of FeCrAlTiY coating consists mainly of Fe and O with a minor amount of Cr and Al. While beneath the aforesaid layer, the oxide is composed of Fe, Cr, Al and O. In accordance with the result of XRD analysis (Figure 8a), the external oxide layer corresponds to Fe_2O_3, mainly. Underneath Fe_2O_3, the oxide layer is probably composed mostly of $Fe(Cr, Al)_2O_4$, as detected in the coating before oxidation. For the FeCrAlTiY coatings with $MoSi_2$ addition, the EDX elemental maps show that the thin external oxide layer is rich in Fe and O, which is estimated as Fe_2O_3. While beneath the Fe_2O_3, the oxide layer consists of Fe, Cr, Al and O which should be $Fe(Cr, Al)_2O_4$. Evidently, from Figure 10, the Fe_2O_3 external layer forms in the FeCrAlTiY coating are thicker compared to that of FeCrAlTiY coatings with $MoSi_2$ addition. This reveals that Fe outward diffusion through spinel oxide is decreased with $MoSi_2$ addition. In addition, the results of EDX elemental maps also show that the formed oxide layer at the coating substrate interface of 20 and 30 $MoSi_2$ coatings contains mainly Fe and O which is suspected to be due to the oxidation of carbon steel substrate as the effect of oxygen inward diffusion through coating pores.

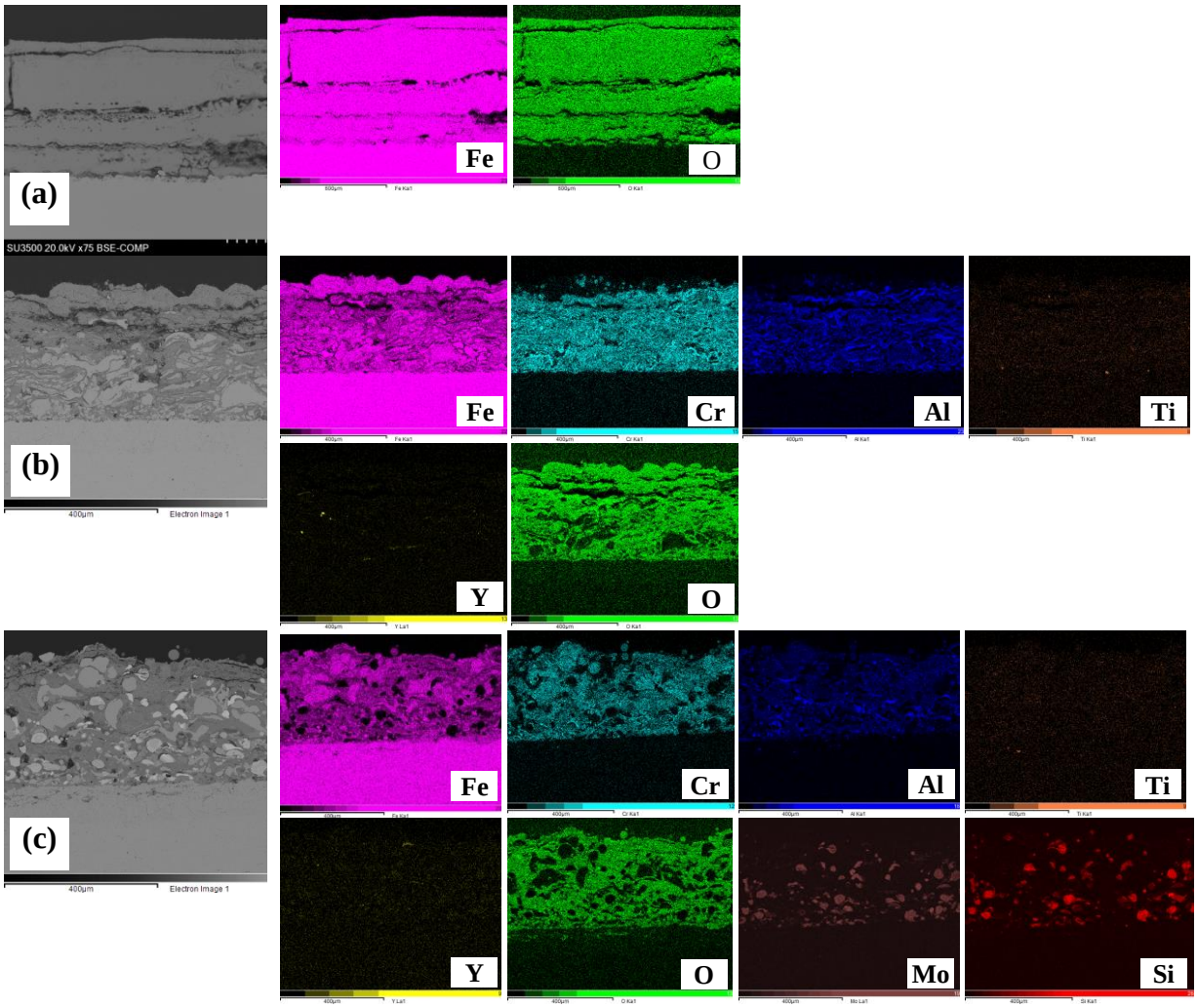

Figure 10 EDX elemental maps of (a) Carbon steel and FeCrAlTiY coatings with (b) 0 and (c) 10 mass% $MoSi_2$ after exposure at 700°C for 8 cycles in air

The obtained results, as shown above, suggest that the FeCrAlTiY-10 mass% $MoSi_2$ coating exhibits the best oxidation resistance after exposure at 700°C for 8 cycles.

4. Conclusions

The evaluation of flame-sprayed FeCrAlTiY with $MoSi_2$ coatings, regarding their oxidizing performance and microstructural evolution, can be summarized as that the $MoSi_2$ content affects the coating microstructure of FeCrAlTiY coatings. The coating becomes more porous with the increase of $MoSi_2$ content. After exposure for 8 cycles at 700°C, FeCrAlTiY coating forms a thick Fe_2O_3 scale. Cracks are also mostly found in the oxide layer and at the oxide/coating interface. These cracks accelerated the oxidizing reactions, resulting the coating degradation. The higher coating porosity observed for FeCrAlTiY coatings with 20 and 30 $MoSi_2$ addition resulted in a preferred path for the oxidizing environment to penetrate the coating, reducing its oxidizing resistance. Among the studied powder mixtures, the FeCrAlTiY-10 $MoSi_2$ has the lowest degradation by oxidizing.

Acknowledgments

This work is supported by Research Center for Advanced Material-National Research and Innovation Agency, Indonesia. The authors also thank Ciswandi and Edi Setiawan for their technical support and discussion.

References

Bennett, M.J., Bull, S.J., 1997. Protection of titanium aluminides by FeCrAlY coatings. *Materials and Corrosion,* Volume 48(1), pp. 48–55

Chakraborty, S.P., 2016. Development of protective coating of $MoSi_2$ over TZM alloy substrate by slurry coating technique. *Materials Today: Proceedings*, Volume 3(9), pp. 3071–3076

Esmaeil, S., Nicolaie, M., Shrikant, J., 2019a. Advances in corrosion-resistant thermal spray coatings for renewable energy power plants. Part I: Effect of composition and microstructure. *Journal of Thermal Spray Technology*, Volume 28, pp. 1749–1788

Esmaeil, S., Nicolaie, M., Shrikant, J., 2019b. Advances in Corrosion-Resistant Thermal Spray Coatings for Renewable Energy Power Plants: Part II—Effect of Environment and Outlook. *J. Therm. Spray Tech.*, Volume 28, pp. 1789–1850

Hansson, K., Halvarsson, M., Tang, J.E., Pompe, R., Sundberg, M., Svensson, J.E., 2004. Protection of Titanium Aluminides by FeCrAlY Coatings. *Journal of the European Ceramic Societ,* Volume 24, pp. 3559–3573

Inoue, Y., Hiraide, N., and Ushioda, K., 2018. Effect of Si addition on oxidation behavior of Nb containing ferritic stainless steel. *ISIJ International*, Volume 58, No. 6, pp. 1117–1125

Ismail, M.I.S., Taha, Z., 2014. Surface hardening of tool steel by plasma arc with multiple passes. *International Journal of Technology*, Volume 5(1), pp. 79–87

Khalesi, F., Farhadian, M., Raeissi, K., 2021. Porosity tailoring of electrophoretically derived zirconia coatings using acidic and alkaline-based sol-gel post-treatment to enhance anti-corrosion performance. *Surface & Coatings Technology*, Volume 425, p. 127692

Luo, X.X., Yao, Z.J., Zhang, P.Z., Miao, Q., Liang, W.P., Wei, D.B., Chen, Y., 2014. A study on high temperature oxidation behavior of double glow plasma surface metallurgy Fe-Al-Cr alloyed layer on Q235 steel. *Applied Surface Science*, Volume 305**,** pp. 259–266

Nikrooz, B., Zandrahimi, M., Ebrahimifar, 2012. High temperature oxidation resistance and corrosion properties of dip coated silica coating by sol gel method on stainless steel. *Journal of Sol-Gel Science and Technology*, Volume 63, pp. 286–293

Saito, Y., Takei, T., Hayashi, S., Yasumori, A., X Okada, H., 1998. Effects of amorphous and crystalline SiO_2 additives on γ-Al_2O_3-to-α-Al_2O_3 phase transitions. *Journal of the American Ceramic Society,* Volume 81(8), pp. 2197–2200

Saraswati, T.E., Nugroho, K., Anwar, M., 2018. An anticorrosion coating from ball-milled wood charcoal and titanium dioxide using a flame spray method. *International Journal of Technology*, Volume 5, pp. 983–992

Simbolon, D.H., Pane. J., Hermanto, B., Afandi, A., Sebayang. K., Situmorang, M., and Sudiro, T., 2020. High temperature oxidation resistance of FeCrAlTiY-MCrAlY (M= Co and Ni) coatings on carbon steel prepared by flame spray technique. *Journal of Protection of Metals and Physical Chemistry of Surfaces*, Volume 58(1), pp. 169–179

Singh S., Kumar R., Goel P., Singh H., 2022. Analysis of Wear and Hardness during Surface Hardfacing of Alloy Steel by Thermal Spraying, Electric Arc and TIG Welding, *Materials Today: Proceedings*, Volume 50, Part 5, pp. 1599-1605

Sofyan, B.T., Berndt, C.C., Stefano, M., Pardede, H.J., 2010. WC-Co coatings for high temperature rocket nozzle applications: An applications note. *International Journal of Technology*. Volume 1(1), pp. 48–56

Tramošljika, B., Blecich, P., Bonefa˘ci´c, I., Glažar, V., 2021. Advanced ultra-supercritical coal-fired power plant with post-combustion carbon capture: analysis of electricity penalty and CO_2 emission reduction. *Sustainability*, Volume 13, 801, pp. 1–20

Wen, S.H., Sha, J.B., 2018. Isothermal and cyclic oxidation behaviours of $MoSi_2$ with additions of B at 1250°C prepared by spark plasma sintering. *Materials Characterization,* Volume 139, pp. 134–143

Wessel, E., Kochubey, V., Naumenko, D., Niewolak, L., Singheiser, L., Quadakkers, W. J., 2004. Effect of Zr addition on the microstructure of the alumina scales on FeCrAlY-Alloys. *Scripta Materialia*, Volume 51, pp. 987–992

Yao, Z., Stiglich, J., Sudarshan, T.S., 1999. Molybdenum silicide based materials and their properties. *Journal of Materials Engineering and Performance,* Volume 8, pp. 291–304

Zhang, L., Tong, Z., He, R., Xie, C., Bai, X., Yang, Y., Fang, D., 2019. Key issues of $MoSi_2$-UHTC ceramics for ultrahigh temperature heating element applications: mechanical, electrical, oxidation and thermal shock behaviors. *Journal of Alloys and Compounds*, Volume 780, pp. 156-163

Zhu, L., Chen, P., Cai, Z-m., Feng, P-z., Kang, X-q., Akhtar, F., Wang, X-h., 2022. Fabrication of $MoSi_2$ coatings on molybdenum and its high-temperature anti-oxidation properties. *Trans. Nonferrous Met. Soc. China*, Volume 32, pp. 935–946